

PREPARED FOR SUBMISSION TO JHEP

Additional Information on Heavy Quark Parameters from Charged Lepton Forward-Backward Asymmetry

Sascha Turczyk^a

^a*PRISMA Cluster of Excellence & Mainz Institute for Theoretical Physics, Johannes Gutenberg University, 55099 Mainz, Germany*

E-mail: turczyk@uni-mainz.de

ABSTRACT: The determination of $|V_{cb}|$ using inclusive and exclusive (semi-)leptonic decays exhibits a long-standing tension of varying $\mathcal{O}(3\sigma)$ significance. For the inclusive determination the decay rate is expanded in $1/m_b$ using heavy quark expansion, and from moments of physical observables the higher order heavy quark parameters are extracted from experimental data in order to assess $|V_{cb}|$ from the normalisation. The drawbacks are high correlations both theoretically as well as experimentally among these observables. We will scrutinise the inclusive determination in order to add a new and less correlated observable. This observable is related to the decay angle of the charged lepton and can help to constrain the important heavy quark parameters in a new way. It may validate the current seemingly stable extraction of $|V_{cb}|$ from inclusive decays or hints to possible issues, and even may be sensitive to New Physics operators.

Contents

1	Introduction	1
2	Decay Rate	3
2.1	Decay Kinematics	3
2.2	Differential Decay Rate	3
2.3	Phase-Space Integration for Forward-Backward Asymmetry	5
2.4	Hadronic Tensor in Heavy Quark Expansion	6
2.5	Integration of the Differential Rate	8
2.6	Effect of Phase-Space Cuts	10
3	Comparison of Expressions to Order $1/m_b^3$	13
4	Numerical Results to Order $1/m_b^5$	16
5	Discussion	20
A	Full Analytic Results to Order $\mathcal{O}(1/m_b^3)$	22

1 Introduction

The cleanest way to access the matrix elements of the Cabibbo-Kobayashi-Maskawa (CKM) matrix are (semi-)leptonic decays [1]. Besides precise experimental data a reliable theoretical framework is necessary. Heavy Quark Symmetry (HQS) and Heavy Quark Expansion (HQE) have proven to be very successful in describing decays of heavy B -mesons [2–5]. Especially in the case of inclusive semi-leptonic decays there has been great effort both from experiment [6–13] and theory [14–17] to push the precision of $|V_{cb}|$ down to $\mathcal{O}(\lesssim 2\%)$ in the global fit [18]. The HQE is a double expansion in $1/m_b$ and α_s . Current state-of-the-art analysis are theoretical calculations up to $\mathcal{O}(\alpha_s^2)$ [19, 20], the mixed $\mathcal{O}(\alpha_s/m_b)$ [21–25] and $\mathcal{O}(1/m_b^5)$ non-perturbative corrections; the results for $1/m_b^3$ have been known [26, 27] for quiet some time, while the calculations of $1/m_b^4$ [28] and $1/m_b^5$ [29] including investigations concerning subtleties due to the heavy final state quark “intrinsic-charm” [30–32] have lately been performed. The most recent global fit [18] uses the theoretical calculations up to $1/m_b^3$ and all known radiative corrections, however the fit results for the extracted $|V_{cb}|$ seem to be rather stable under adding higher order theoretical corrections as can be seen from older global analysis [33–35]. The number of new parameters at order $1/m_b^{4,5}$ proliferates, and hence these results cannot be simply implemented into the fit to experimental data. Some numerical studies about the effects and possible extraction of some of the most important parameters are ongoing [36], using partially estimates of these higher-order matrix elements [37].

The higher precision and especially accumulated data of the future Belle-II experiment [38] will be able to make use out of this additional and less correlated observable. It will hopefully help to disentangle the tension with respect to the extraction of $|V_{cb}|$ utilising other methods or may contribute to solve some other puzzles in this decay mode [39]. It has been noted before [40, 41], that right-handed currents may help to ease this tension, especially in $b \rightarrow u$ transitions. The relation between the transition to the heavy charm quark or light up quark is however model-dependent. First studies have estimated the potential impact of right-handed currents both in inclusive [42–44] as well as exclusive $b \rightarrow c\ell\bar{\nu}_\ell$ transitions [45], still allowing for a few percent of a right-handed current admixture. A recent LHCb analysis [46] using a baryonic decay mode disfavours this New Physics (NP) interpretation of the tension in $b \rightarrow u$ transitions¹, while there has been a possible solution prior to this measurement [47].

We believe the statement of [48] that right-handed currents in $b \rightarrow u(c)$ semi-leptonic transitions are already ruled out by data is too strong. Their motivation to exclude right-handed currents in $b \rightarrow u$ transitions bases purely on the reinterpretation of the $B \rightarrow \rho\ell\bar{\nu}_\ell$ measurement. Besides issues with experimentally identifying the broad ρ -resonance [49, 50] in accordance with its theory description especially for the normalisation, their reinterpretation of experimental data integrated over a range of q^2 into a single value of q^2 outside of this region does neither take into account efficiency corrections of the altered q^2 spectrum due to NP contributions, nor uses it the theoretical non-perturbative predictions at a point in phase-space, where these are valid and the uncertainties are trustworthy. Therefore neither the central value nor the uncertainty band as a function of the right-handed admixture are computed reliably. Hence their conclusion to exclude right-handed currents purely to a deviation from their derived uncertainty band at the one sigma level is too strong. In a first order approximation in [47] we have taken into account such effects to reinterpret the Neyman belt using the same experimental data, in the valid theoretical range of low q^2 for the form factor predictions. In this analysis right-handed currents may not be excluded, yet. It is obvious, that a correct exclusion calls for a revisit of the measurements with taking into account efficiency and acceptance corrections for the NP altered spectrum. The statement for the $b \rightarrow c$ transition is less severe. Furthermore even in the purely exclusive extraction there exist still a discrepancy using either light-cone sum rules or lattice QCD [1]. Hence there cannot be a conclusive decision made with the current theoretical and experimental situation, and therefore we think the line of argumentation in [48] is too restrictive.

We neglect lepton masses in the following discussion. The paper is organised as follows. In section 2, we will derive the differential spectrum and the forward-backward asymmetry and discuss subtleties due to introducing a cut of the minimum energy for the charged lepton. Section 3 provides the expressions up to order $\mathcal{O}(1/m_b^3)$ to demonstrate the use and additional information of this observable in comparison to moments of the hadronic invariant mass and charged lepton energy. In Section 4 we will discuss the impact of higher-orders numerically, where full results are available analytically, and conclude in Section 5.

¹Note that this measurement of $|V_{ub}|$ depends on the value of $|V_{cb}|$, which has been fixed to the value extracted from exclusive semi-leptonic decays. Using the inclusive value for $|V_{cb}|$, the extracted central value of $|V_{ub}|$ would be larger by about 7%.

2 Decay Rate

2.1 Decay Kinematics

For the following discussion to be useful in analysis, we assume that the full event kinematics may be reconstructed experimentally. That can be achieved at (Super-) B -factories [38] with hadronic tag analysis to reconstruct the kinematics including the invisible neutrino momentum. This decay kinematics is given by

$$p_B^\mu = p_\ell^\mu + p_{\bar{\nu}_\ell}^\mu + p_{x_C}^\mu := q^\mu + p_{x_C}^\mu. \quad (2.1)$$

Here q^μ is the momentum transfer to the lepton system, and $p_B^\mu = m_B v^\mu$ with v^μ being the four velocity of the B -meson, and $(v^\mu) = (1, 0, 0, 0)$ in the B -meson rest-frame. We calculate the fully differential rate in the three kinematical variables

$$q^2 = 2p_\ell \cdot p_{\bar{\nu}_\ell} \quad (2.2a)$$

$$v \cdot q = v \cdot p_\ell + v \cdot p_{\bar{\nu}_\ell} \quad (2.2b)$$

$$z := \cos \theta = \frac{v \cdot p_{\bar{\nu}_\ell} - v \cdot p_\ell}{\sqrt{v \cdot q^2 - q^2}}. \quad (2.2c)$$

The angle $z = \cos \theta$ is defined the same way as for the forward-backward asymmetry [51] A_{FB} in the flavor changing neutral current decay $b \rightarrow s \ell^+ \ell^-$: it is given by the angle of the charged lepton with the flight direction of the B -meson, in the rest-frame of the lepton-anti-neutrino system ($\vec{q} = 0$). As given in Eq. (2.2c) it can be related to the energies of both leptons and the momentum transfer to the lepton system in the B -rest-frame. In this form it can be seen that z is a Lorentz invariant observable. All other possible contractions of appearing four momentum vectors depend linearly on the choice of (2.2).

2.2 Differential Decay Rate

The differential rate can be decomposed into the leptonic and hadronic tensor

$$d\Gamma = 16\pi G_F^2 |V_{cb}|^2 W_{\mu\nu} L^{\mu\nu} d\phi, \quad (2.3)$$

where we have defined the leptonic and hadronic tensor as

$$L^{\mu\nu} = \sum_{\substack{\text{lepton} \\ \text{spins}}} \langle 0 | J_\ell^{\nu\dagger} | \ell \bar{\nu}_\ell \rangle \langle \ell \bar{\nu}_\ell | J_\ell^\mu | 0 \rangle \quad (2.4)$$

$$W_{\mu\nu} = \frac{1}{2m_B} \sum_{X_c} \langle \bar{B} | J_{q,\nu}^\dagger | X_c \rangle \langle X_c | J_{q,\mu} | \bar{B} \rangle (2\pi)^3 \delta^{(4)}(p_B - (p_\ell + p_{\bar{\nu}_\ell} + p_{X_c})), \quad (2.5)$$

and used the abbreviation for the Standard Model (SM) quark and hadronic current

$$J_\ell^\mu = \bar{\ell} \gamma^\mu \frac{1 - \gamma^5}{2} \nu_\ell \quad (2.6)$$

$$J_{q,\mu} = \bar{c} \gamma_\mu \frac{1 - \gamma^5}{2} b. \quad (2.7)$$

In case of a previously mentioned right-handed admixture, we would have

$$J_{q,\mu}^{\text{NP}} = \bar{c}\gamma_\mu \frac{1-\gamma^5}{2} b + \epsilon_R \bar{c}\gamma_\mu \frac{1+\gamma^5}{2} b, \quad (2.8)$$

and need to redefine $V_{cb} \rightarrow V_{cb}^L$. As far as the decay kinematics is concerned, we may use the three invariants $v \cdot q$, q^2 as well as $z = \cos \theta$. The latter one has not been considered in tree-level decays, yet. It has been used in flavor changing neutral currents though [51], in which New Physics is suspected to show off first as it may enter at the same order as the Standard Model contribution and both leptons are charged and thus experimentally visible. As we will later see, we treat the hadronic part in heavy quark effective theory (HQET). Then the b -quark momentum is given by $p_b^\mu = m_b v^\mu + k^\mu$, where the soft vector k^μ describes the off-shellness of the heavy quark. Basically we expand the hadronic tensor in powers of k^μ , using a background field method with $k^\mu \rightarrow iD^\mu$, in a systematic way in order to preserve the correct ordering [28]. Thus we treat the decay phase-space at partonic level kinematics, i.e.

$$p_b^\mu = m_b v^\mu + k^\mu = q^\mu + p_c^\mu. \quad (2.9)$$

The off-shellness of the bottom quark will be mimicked by derivatives of the on-shell delta distribution condition of the hadronic tensor, which occurs at higher orders in the $1/m_b$ expansion. This however, has no impact on the leptonic side, as we can factorise the decay rate according to Eq. (2.3) and we have

$$d\Gamma = 16\pi G_F^2 |V_{cb}|^2 \tilde{W}_{\mu\nu} \tilde{L}^{\mu\nu} \quad (2.10a)$$

$$\begin{aligned} \tilde{W}_{\mu\nu} &= \int \frac{ds}{2\pi} \frac{d^4q}{(2\pi)^4} 2\pi\delta(s - q^2) W_{\mu\nu} \\ &= \frac{1}{8\pi^3} \sqrt{v \cdot q^2 - q^2} W_{\mu\nu} dq^2 dv \cdot q \end{aligned} \quad (2.10b)$$

$$\tilde{L}^{\mu\nu} = \int \frac{d^3p_\ell}{(2\pi)^3 2E_\ell} \frac{d^3p_{\bar{\nu}_\ell}}{(2\pi)^3 2E_{\bar{\nu}_\ell}} L^{\mu\nu} (2\pi)^4 \delta^{(4)}(q - p_\ell - p_{\bar{\nu}_\ell}). \quad (2.10c)$$

The hadronic tensor can be decomposed into structure functions depending each only on $v \cdot q$ and q^2

$$W_{\mu\nu} = -g_{\mu\nu} W_1 + v_\mu v_\nu W_2 - i\epsilon_{\mu\nu\alpha\beta} v^\alpha q^\beta W_3 + q_\mu q_\nu W_4 + (v_\mu q_\nu + v_\nu q_\mu) W_5. \quad (2.11)$$

The leptonic tensor is simply given by

$$L^{\mu\nu} = 2 \left(p_\ell^\mu p_{\bar{\nu}_\ell}^\nu + p_{\bar{\nu}_\ell}^\nu p_\ell^\mu - g^{\mu\nu} p_\ell \cdot p_{\bar{\nu}_\ell} - i\epsilon^{\mu\nu\eta\lambda} p_{\ell\eta} p_{\bar{\nu}_\ell\lambda} \right). \quad (2.12)$$

The contraction of the leptonic tensor and hadronic tensor in turn is then given by

$$L^{\mu\nu} W_{\mu\nu} = 2q^2 W_1 + (1 - z^2) (v \cdot q^2 - q^2) W_2 + 2q^2 z \sqrt{v \cdot q^2 - q^2} W_3. \quad (2.13)$$

As can be seen from this equation, the contribution from W_3 is sensitive to asymmetric integrations over z , which for example is true in observables as a forward-backward asymmetry, while the other two terms with $W_{1,2}$ drop out. In contrast for the regular integration

over the whole kinematically allowed region of z , as done for all “conventional” observables, the contribution from W_3 drops out and we are purely sensitive to $W_{1,2}$. Hence we are interested in constructing the observable such, that we gain additional information on W_3 , which is otherwise lost.

The decomposition we have elaborated on in Eq. (2.10) enables us to calculate the phase-space for the triple differential decay rate in the following subsection.

2.3 Phase-Space Integration for Forward-Backward Asymmetry

By construction the dependence of $v \cdot q$ and q^2 is contained in the hadronic tensor. We need to perform the phase-space integration over the leptonic degrees of freedom including the leptonic tensor with implicitly retaining the dependence on the angle z . Strictly speaking, the phase-space integration is only valid for the full contraction of the hadronic tensor with the leptonic tensor given by Eq. (2.13), which we keep in mind in the following². This contraction does depend only on the three kinematic variables in Eq. (2.2), and due to the hadronic part in Eq. (2.10b) we are already differential in $v \cdot q$ and q^2 . We calculate the phase-space for massless leptons, and we introduce the dependence on the angular variable explicitly

$$\begin{aligned}
\int d\phi &= \int \frac{d^3 p_\ell}{(2\pi)^3 2E_\ell} \frac{d^4 p_\nu}{(2\pi)^4} (2\pi) \delta(p_\nu^2) (2\pi)^4 \delta(q - p_\nu - p_\ell) \theta(p_\nu^0) \\
&\quad \times dz \delta\left(z - \frac{p_\nu^0 - p_\ell^0}{\sqrt{v \cdot q^2 - q^2}}\right) \theta(E_\ell - E_{\text{cut}}) \\
&= \int \frac{d\Omega_\ell}{(2\pi)^2} \frac{E_\ell^2 dE_\ell}{2E_\ell} dz \delta\left((q - p_\ell)^2\right) \delta\left(z - \frac{v \cdot q - 2E_\ell}{\sqrt{v \cdot q^2 - q^2}}\right) \theta(E_\ell - E_{\text{cut}}) \theta(v \cdot q - E_\ell) \\
&= \int \frac{d \cos \theta_\ell}{2\pi} \frac{dE_\ell}{4\sqrt{v \cdot q^2 - q^2}} \delta\left(\cos \theta_\ell - \frac{2E_\ell v \cdot q - q^2}{2E_\ell \sqrt{v \cdot q^2 - q^2}}\right) \theta(1 + \cos \theta_\ell) \theta(1 - \cos \theta_\ell) \\
&\quad \times dz \frac{\sqrt{v \cdot q^2 - q^2}}{2} \delta\left(E_\ell - \frac{1}{2}(v \cdot q - z \sqrt{v \cdot q^2 - q^2})\right) \theta(E_\ell - E_{\text{cut}}) \theta(v \cdot q - E_\ell) \\
&= \frac{dz}{16\pi} \theta(q^2) \theta(v \cdot q^2 - q^2) \theta(v \cdot q - z \sqrt{v \cdot q^2 - q^2} - 2E_{\text{cut}}). \tag{2.14}
\end{aligned}$$

The angle $\cos \theta_\ell$ shall not be confused with the observable $z = \cos \theta$. In deriving this result, we have used

$$\begin{aligned}
(q - p_\ell)^2 &= q^2 - 2q \cdot p_\ell \\
&= q^2 - 2(v \cdot q E_\ell - |\vec{q}| |\vec{p}_\ell| \cos \theta_\ell) \\
&= q^2 - 2v \cdot q E_\ell + 2E_\ell \sqrt{v \cdot q^2 - q^2} \cos \theta_\ell \\
\Rightarrow \delta\left((q - p_\ell)^2\right) &= \frac{1}{2E_\ell \sqrt{v \cdot q^2 - q^2}} \delta\left(\cos \theta_\ell - \frac{2E_\ell v \cdot q - q^2}{2E_\ell \sqrt{v \cdot q^2 - q^2}}\right). \tag{2.15}
\end{aligned}$$

²Alternatively we may decompose $I_{\mu\nu}(v \cdot q, q^2, z) = \int d\phi L_{\mu\nu}$ into leptonic structure functions. However then we were not be able to identify the z dependence, which multiplies the hadronic structure functions in Eq (2.13), because it is only contained in $I_{\mu\nu}$ due to its relation with the leptonic phase-space.

In the last step we have evaluated the integrals using the delta distributions. For applying this to the lepton angle, we needed to introduce further theta distributions to limit the integration region of $\cos\theta_\ell$ to the physical ones. Then we have simplified the kinematical constraints of the theta distributions, and we will later see that these distributions are necessary for the derivation of integrated observables. Trivial conditions may be neglected.

In summary the triple differential decay rate is written as

$$\begin{aligned} \frac{d^3\Gamma}{dv\cdot q dq^2 dz} &= \frac{G_F^2 |V_{cb}|^2}{192\pi^3 m_b^5} 24m_b^5 \sqrt{v\cdot q^2 - q^2} \\ &\times \left[2q^2 W_1 + (1 - z^2) (v\cdot q^2 - q^2) W_2 + 2zq^2 \sqrt{v\cdot q^2 - q^2} W_3 \right] \\ &\times \theta(q^2)\theta(v\cdot q^2 - q^2)\theta(v\cdot q - z\sqrt{v\cdot q^2 - q^2} - 2E_{\text{cut}}). \end{aligned} \quad (2.16)$$

2.4 Hadronic Tensor in Heavy Quark Expansion

We proceed along the lines of [29] to compute the hadronic tensor in the HQE, which we shall briefly summarise here. We start with a non-local forward matrix element of the form

$$T_{\mu\nu} = -\frac{i}{2M_B} \int d^4x e^{-iqx} \langle \bar{B} | T [J_{q,\nu}^\dagger(x), J_{q,\mu}(0)] | \bar{B} \rangle. \quad (2.17)$$

This can be visualised by the Feynman diagram in Fig. 1. The double line denotes the

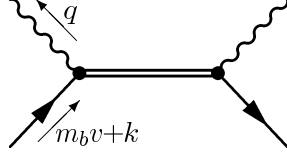


Figure 1. Background field propagator.

charm quark that propagates in the soft background fields of the meson. We relate this time-ordered product to the hadronic tensor by the optical theorem

$$-\frac{1}{\pi} \text{Im} T_{\mu\nu} = \frac{1}{2M_B} \sum_{X_c} \langle \bar{B} | J_{q,\nu}^\dagger | X_c \rangle \langle X_c | J_{q,\mu} | \bar{B} \rangle (2\pi)^3 \delta^4(p_B - q - p_{X_c}) = W_{\mu\nu}. \quad (2.18)$$

The soft momentum k of the momentum transfer $p_b - q$ from Eq. (2.9) is replaced by the covariant derivative in the charm quark propagator, containing the soft background field gluons. This propagator then becomes the background field (BGF) propagator

$$S_{\text{BGF}} = \frac{1}{m_b \not{v} + i\not{D} - \not{q} - m_c + i\epsilon}. \quad (2.19)$$

The BGF propagator describes the charm quark propagating in the forward matrix element of the B -meson with all the soft fields, for instance binding gluons, and therefore accounts for the difference between the partonic quark picture and the non-perturbative nature of the meson. We write this non-local propagator as a geometric series, to yield an expansion in k^μ/m_b with $Q^\mu = m_b v^\mu - q^\mu$

$$S_{\text{BGF}} = \left[\sum_{n=0}^{\infty} (-1)^n \left[(Q - m_c + i\epsilon)^{-1} (i\not{D}) \right]^n \right] (Q - m_c)^{-1} \quad (2.20)$$

and the operator product expansion (OPE) can be cut off at some mass dimension m . In our case we compute up to $m = 5$, which yields the expansion up to $1/m_b^5$. Notice that the application of the optical theorem

$$-\frac{1}{\pi}\text{Im} T_{\mu\nu} = W_{\mu\nu}, \quad (2.21)$$

can be evaluated explicitly by the means of

$$-\frac{1}{\pi}\text{Im} \left(\frac{1}{\Delta_0} \right)^{n+1} = \frac{(-1)^n}{n!} \delta^{(n)}(Q^2 - m_c^2), \quad (2.22)$$

and we have defined $\Delta_0 = Q^2 - m_c^2 + i\epsilon$. Thus we find derivatives of the on-shell condition for the higher-order terms, reassembling the non-locality of the unexpanded BGF propagator into local terms. In this procedure the full QCD field in the OPE is retained and we are left with only local operators. No additional non-local pieces from expanding the state as well as the field will occur, however the relation to other heavy hadrons containing a heavy quark is now only true up to corrections of order $1/m_Q$ and α_s . To coincide with the usually defined parameters in dimension 5, which is equal to expanding up to $1/m_b^2$, we define the operators to be

$$2M_B \mu_\pi^2 = -\langle \bar{B} | \bar{b}_v iD_\rho iD_\sigma b_v | \bar{B} \rangle \Pi^{\rho\sigma} \quad (2.23a)$$

$$2M_B \mu_G^2 = \frac{1}{2} \langle \bar{B} | \bar{b}_v [iD_\rho, iD_\sigma] (-i\sigma_{\alpha\beta}) b_v | \bar{B} \rangle \Pi^{\alpha\rho} \Pi^{\beta\sigma}. \quad (2.23b)$$

Here $\Pi_{\mu\nu} \equiv v_\mu v_\nu - g_{\mu\nu}$ is the projector onto the spatial components. We can identify μ_π^2 with the kinetic energy term and μ_G^2 as the chromo-magnetic moment. In dimension 6, corresponding to $1/m_b^3$ we define the Darwin term ρ_D^3 and the spin-orbit term ρ_{LS}^3 as

$$2M_B \rho_D^3 = \frac{1}{2} \langle \bar{B} | \bar{b}_v [iD_\rho, [iD_\sigma, iD_\lambda]] b_v | \bar{B} \rangle \Pi^{\rho\lambda} v^\sigma \quad (2.24a)$$

$$2M_B \rho_{LS}^3 = \frac{1}{2} \langle \bar{B} | \bar{b}_v \left\{ iD_\rho, [iD_\sigma, iD_\lambda] \right\} (-i\sigma_{\mu\nu}) b_v | \bar{B} \rangle \Pi^{\alpha\rho} \Pi^{\beta\lambda} v^\sigma. \quad (2.24b)$$

There appear 9 additional parameters m_1, \dots, m_9 in dimension 7 corresponding to $1/m_b^4$, and 18 in dimension 8, which we label r_1, \dots, r_{18} . Their definition may be found in [29].

In summary, the hadronic structure tensor is written as

$$\begin{aligned}
W_{\mu\nu} &= -\frac{1}{\pi} \text{Im} \langle B(p) | \bar{b}_\nu \Gamma_\nu^\dagger i S_{\text{BGF}} \Gamma_\mu b_\nu | B(p) \rangle \\
&= \sum_i \text{Tr} \left\{ \Gamma_\nu^\dagger (\mathcal{Q} + m_c) \Gamma_\mu \hat{\Gamma}^{(i)} \right\} A^{(i,0)} \delta(Q^2 - m_c^2) \\
&+ \sum_i \text{Tr} \left\{ \Gamma_\nu^\dagger (\mathcal{Q} + m_c) \gamma^{\mu_1} (\mathcal{Q} + m_c) \Gamma_\mu \hat{\Gamma}^{(i)} \right\} A_{\mu_1}^{(i,1)} \delta^{(1)}(Q^2 - m_c^2) \\
&+ \sum_i \text{Tr} \left\{ \Gamma_\nu^\dagger (\mathcal{Q} + m_c) \gamma^{\mu_1} (\mathcal{Q} + m_c) \gamma^{\mu_2} (\mathcal{Q} + m_c) \Gamma_\mu \hat{\Gamma}^{(i)} \right\} A_{\mu_1 \mu_2}^{(i,2)} \frac{\delta^{(2)}(Q^2 - m_c^2)}{2} \\
&+ \dots \\
&+ \sum_i \text{Tr} \left\{ \Gamma_\nu^\dagger (\mathcal{Q} + m_c) \gamma^{\mu_1} (\mathcal{Q} + m_c) \cdot \dots \cdot (\mathcal{Q} + m_c) \gamma^{\mu_m} (\mathcal{Q} + m_c) \Gamma_\mu \hat{\Gamma}^{(i)} \right\} A_{\mu_1 \mu_2 \dots \mu_m}^{(i,m)} \\
&\quad \times \frac{\delta^{(m)}(Q^2 - m_c^2)}{m!}. \tag{2.25}
\end{aligned}$$

The coefficients $A_{\mu_1 \mu_2 \dots \mu_m}^{(i,m)}$ are known analytically up to order $1/m_b^5$ ($m = 5$) [29]. In the next subsection, we will see the impact of the kinematic limits from the theta distributions in (2.16) for higher order terms. Therefore we can write the triple differential rate as

$$\frac{d^3\Gamma}{dv \cdot Q dQ^2 dz} = \sum_{n=0}^5 \frac{d^3\Gamma^{(n)}}{dv \cdot Q dQ^2 dz} \delta^{(n)}(Q^2 - m_c^2). \tag{2.26}$$

2.5 Integration of the Differential Rate

For the evaluation of the on-shell condition, it is advantageous to perform a variable transformation as we have already indicated above to simplify the BGF propagator

$$Q^\mu = m_b v^\mu - q^\mu \tag{2.27a}$$

$$v \cdot q = m_b - v \cdot Q \tag{2.27b}$$

$$q^2 = m_b^2 - 2m_b v \cdot Q + Q^2 \tag{2.27c}$$

$$\Rightarrow v \cdot q^2 - q^2 = v \cdot Q^2 - Q^2 \tag{2.27d}$$

$$dv \cdot q dq^2 = dv \cdot Q dQ^2. \tag{2.27e}$$

Effectively Q is the momentum of the final state X_c system, while q is the kinematics from the lepton system. Then the delta distribution in the hadronic structure functions simplifies to

$$\delta^{(n)}((m_b v - q)^2 - m_c^2) \rightarrow \delta^{(n)}(Q^2 - m_c^2). \tag{2.28}$$

As a consequence the delta distribution does depend only on a single variable. Hence it is easiest to perform first the integration on $v \cdot Q$. From (2.16) we find the two conditions

$$\theta(q^2) \theta(v \cdot q^2 - q^2) = \theta(m_b^2 - 2m_b v \cdot Q + q^2) \theta(v \cdot Q^2 - Q^2), \tag{2.29}$$

where we have neglected the effect on the lepton energy cut, which we shall investigate below. From this it is straight-forward to compute the double differential rate

$$\frac{d^2\Gamma^{(n)}}{dQ^2 dz} = \int_{\sqrt{Q^2}}^{\frac{m_b^2+Q^2}{2m_b}} dv \cdot Q \frac{d^3\Gamma^{(n)}}{dv \cdot Q dQ^2 dz}. \quad (2.30)$$

The angular spectrum is now obtained by partially integrating Eq. (2.30) in Q^2 to evaluate the delta distribution

$$\frac{d\Gamma}{dz} = \sum_{n=0}^5 (-1)^n \frac{d^n}{d(Q^2)^n} \frac{d^2\Gamma^{(n)}}{dQ^2 dz} \Big|_{Q^2=m_e^2}. \quad (2.31)$$

Now as far as this spectrum is concerned, we have several choices, which we will investigate in turn.

1. First we integrate to the total rate as a cross-check with the known result [29] to verify our procedure

$$\Gamma = \int_{-1}^1 dz \frac{d\Gamma}{dz}. \quad (2.32)$$

2. We can analyse the differential spectrum $\frac{d\Gamma}{dz}$ itself.
3. We can construct the forward backward asymmetry

$$A_{FB} = \frac{\int_{-1}^0 dz \frac{d\Gamma}{dz} - \int_0^1 dz \frac{d\Gamma}{dz}}{\int_{-1}^1 dz \frac{d\Gamma}{dz}}. \quad (2.33)$$

4. It is possible to construct moments of the angular distribution

$$\langle z^n \rangle_{\pm} = \frac{\int_{-1}^0 dz z^n \frac{d\Gamma}{dz} \pm \int_0^1 dz z^n \frac{d\Gamma}{dz}}{\int_{-1}^1 dz \frac{d\Gamma}{dz}}. \quad (2.34)$$

We will analyse the differential spectrum itself and the A_{FB} in sections 3 and 4. Note that we do not gain much more information from the moments $\langle z^n \rangle_{\pm}$, as can be inferred from Eq. (2.16), because z is a polynomial prefactor of the structure functions and without the electron energy cut there is no additional constraint. For illustration, we will compare even and odd moments with $m \in \mathbb{N}$

$$\langle z^{2m} \rangle_+ \propto \frac{2}{2m+1} \left(W_1 - \frac{2}{2m+3} W_2 \right) \quad (2.35a)$$

$$\langle z^{2m} \rangle_- \propto -\frac{2}{2m+2} W_3 \quad (2.35b)$$

$$\langle z^{2m+1} \rangle_+ \propto \frac{2}{2m+3} W_3 \quad (2.35c)$$

$$\langle z^{2m+1} \rangle_- \propto -\frac{2}{2m+2} \left(W_1 - \frac{2}{2m+3} \frac{2m+3}{2m+4} W_2 \right). \quad (2.35d)$$

It is obvious, that we cannot gain more information on W_3 from moments in z . We would generate with higher even moments in z for the total rate a different linear combination for W_1 and W_2 , which is a bit different but very similar for odd moments in z of the forward backward asymmetry. As experimental uncertainties are growing for the measurement of higher moments and the theoretical correlation is large with the linear combinations being similar for various moments, it is probably not worthwhile to study moments in z in detail. Furthermore the moments already taken into account are linear combinations of $W_{1,2}$.

2.6 Effect of Phase-Space Cuts

As we can see in Eq. (2.16), the introduction of a charged lepton energy cut introduces a non-trivial dependence into the phase-space integration. The additional conditions

$$0 \leq m_b - v \cdot Q - z \sqrt{v \cdot Q^2 - Q^2} - 2E_{\text{cut}} \quad (2.36a)$$

$$0 \leq E_{\text{cut}} \leq \frac{m_b^2 - mc^2}{2} = E_\ell^{\text{max}} \quad (2.36b)$$

and the already previously appearing limits

$$Q^2 \leq v \cdot Q \quad (2.37a)$$

$$0 \leq m_b^2 - 2m_b v \cdot Q + Q^2 \quad (2.37b)$$

$$-1 \leq z \leq 1 \quad (2.37c)$$

will restrict the allowed integration region into several parts. We first need to split the regions for two conditions, where in region I the constraint from (2.36) is always fulfilled, while in region II, we have to cut into the phase-space of $v \cdot Q$ and z

$$\frac{1}{2} \left(m_b - v \cdot Q - \sqrt{v \cdot Q^2 - Q^2} \right) \geq E_{\text{cut}} \geq 0 \quad \text{Region I} \quad (2.38a)$$

$$\frac{1}{2} \left(m_b - v \cdot Q - \sqrt{v \cdot Q^2 - Q^2} \right) \leq E_{\text{cut}} \leq E_\ell^{\text{max}} \quad \text{Region II.} \quad (2.38b)$$

For region I we find from Eq. (2.38a) a different upper limit for the $v \cdot Q$ integration than without a cut

$$\sqrt{v \cdot Q} \leq v \cdot Q \leq \frac{4E_{\text{cut}}m_b - m_b^2 - 4E_{\text{cut}}^2 - Q^2}{2(2E_{\text{cut}} - m_b)}. \quad (2.39)$$

The constraint for the z integration in region I is obviously the same as in the case without the minimum electron energy cut, as the additional condition depending on z is always fulfilled.

Now for region II we find from Eq. (2.36a) a minimum value for

$$v \cdot Q \geq \frac{4E_{\text{cut}}m_b - m_b^2 - 4E_{\text{cut}}^2 - Q^2}{2(2E_{\text{cut}} - m_b)} \quad (2.40)$$

by examining the extreme values for the angle $z = \pm 1$, while for decreasing $|z| < 1$ the condition is relaxed. We therefore find a separation in z , up to which we are allowed to integrate over the full phase-space $v \cdot Q \leq \frac{m_b^2 + Q^2}{2m_b}$

$$-1 \leq z \leq \frac{-4E_{\text{cut}}m_b + m_b^2 - Q^2}{m_b^2 - Q^2}. \quad (2.41)$$

For the remaining integration over the the angle

$$\frac{-4E_{\text{cut}}m_b + m_b^2 - Q}{m_b^2 - Q} \leq z \leq 1 \quad (2.42)$$

we find a maximal allowed value for

$$v \cdot Q \leq \frac{mb - 2E_{\text{cut}} - |z|\sqrt{(m_b - 2E_{\text{cut}})^2 + Q^2(z^2 - 1)}}{1 - z^2}. \quad (2.43)$$

Note, that region I reduces to the usual integration in the limit $E_{\text{cut}} \rightarrow 0$, while region II moves out of the allowed region and hence does not contribute and we recover the previous case. So in summary, we find three integration regions, where in part there are non-trivial dependencies among the integration variables. The constraints are given by

Region I.A:

$$\begin{aligned} \sqrt{Q^2} \leq v \cdot Q \leq \frac{4E_{\text{cut}}m_b - m_b^2 - 4E_{\text{cut}}^2 - Q^2}{2(2E_{\text{cut}} - m_b)} \\ -1 \leq z \leq 1. \end{aligned} \quad (2.44a)$$

Region II.B:

$$\begin{aligned} \frac{4E_{\text{cut}}m_b - m_b^2 - 4E_{\text{cut}}^2 - Q^2}{2(2E_{\text{cut}} - m_b)} \leq v \cdot Q \leq \frac{m_b^2 + Q^2}{2m_b} \\ -1 \leq z \leq \frac{-4E_{\text{cut}}m_b + m_b^2 - m_c^2}{m_b^2 - m_c^2} := z_{\text{cut}}. \end{aligned} \quad (2.44b)$$

Region II.C:

$$\begin{aligned} \frac{4E_{\text{cut}}m_b - m_b^2 - 4E_{\text{cut}}^2 - Q^2}{2(2E_{\text{cut}} - m_b)} \leq v \cdot Q \leq \frac{mb - 2E_{\text{cut}} - |z|\sqrt{(m_b - 2E_{\text{cut}})^2 + Q^2(z^2 - 1)}}{1 - z^2} \\ z_{\text{cut}} := \frac{-4E_{\text{cut}}m_b + m_b^2 - m_c^2}{m_b^2 - m_c^2} \leq z \leq 1. \end{aligned} \quad (2.44c)$$

In the following we will restrict the cut separation in z

$$z_{\text{cut}} = \frac{-4E_{\text{cut}}m_b + m_b^2 - m_c^2}{m_b^2 - m_c^2} \quad (2.45)$$

such, that this quantity is positive for reasons that will become obvious. Consequently we have $|z| = z$ in region II.C, which will be used below. Then

$$0 \leq E_{\text{cut}} \leq \frac{m_b^2 - m_c^2}{4m_b} \approx 1.08 \text{ GeV}. \quad (2.46)$$

For the numerical estimate we have used the latest fit results in [18]. The analysis with an even larger charged lepton energy cut would in principle be the same, however some of the contributions for the forward-backward asymmetry would shift between the positive and

negative term. As a realistic cut from current analysis is $E_{\text{cut}} \lesssim 1$ GeV or maybe below for future analysis³, this is a good starting point. However the constraint should be kept in mind and fits, if not both masses are taken from other sources as already done for the charm quark mass [18], should be verified afterwards to fulfil this condition in order to check if the predictions for A_{FB} actually match.

Therefore the double differential rates in the three regions are obtained by the integrals

$$\frac{d^2\Gamma_A^{(n)}}{dQ^2 dz} = \int_{\sqrt{Q^2}}^{\frac{4E_{\text{cut}}m_b - m_b^2 - 4E_{\text{cut}}^2 - Q^2}{2(2E_{\text{cut}} - m_b)}} dv \cdot Q \frac{d^3\Gamma^{(n)}}{dv \cdot Q dQ^2 dz} \quad (2.47a)$$

$$\frac{d^2\Gamma_B^{(n)}}{dQ^2 dz} = \int_{\frac{m_b^2 + Q^2}{2m_b}}^{\frac{4E_{\text{cut}}m_b - m_b^2 - 4E_{\text{cut}}^2 - Q^2}{2(2E_{\text{cut}} - m_b)}} dv \cdot Q \frac{d^3\Gamma^{(n)}}{dv \cdot Q dQ^2 dz} \quad (2.47b)$$

$$\frac{d^2\Gamma_C^{(n)}}{dQ^2 dz} = \int_{\frac{4E_{\text{cut}}m_b - m_b^2 - 4E_{\text{cut}}^2 - Q^2}{2(2E_{\text{cut}} - m_b)}}^{\frac{m_b - 2E_{\text{cut}} - |z|\sqrt{(m_b - 2E_{\text{cut}})^2 + Q^2(z^2 - 1)}}{1 - z^2}} dv \cdot Q \frac{d^3\Gamma^{(n)}}{dv \cdot Q dQ^2 dz} . \quad (2.47c)$$

The difficulty now comes into the game, as we have to take into account the additional constraints on z for regions B and C , see Eq. (2.44). The angular spectrum is obtained by

$$\frac{d\Gamma_A}{dz} = \sum_{n=0}^5 (-1)^n \frac{d^n}{d(Q^2)^n} \frac{d^2\Gamma_A^{(n)}}{dQ^2 dz} \Big|_{Q^2=m_c^2} \quad (2.48a)$$

$$\frac{d\Gamma_B}{dz} = \sum_{n=0}^5 (-1)^n \frac{d^n}{d(Q^2)^n} \left[\frac{d^2\Gamma_B^{(n)}}{dQ^2 dz} \theta \left(\frac{-4E_{\text{cut}}m_b + m_b^2 - Q^2}{m_b^2 - Q^2} - z \right) \right]_{Q^2=m_c^2} \quad (2.48b)$$

$$\frac{d\Gamma_C}{dz} = \sum_{n=0}^5 (-1)^n \frac{d^n}{d(Q^2)^n} \left[\frac{d^2\Gamma_C^{(n)}}{dQ^2 dz} \theta \left(-\frac{-4E_{\text{cut}}m_b + m_b^2 - Q^2}{m_b^2 - Q^2} + z \right) \right]_{Q^2=m_c^2} . \quad (2.48c)$$

So we see, that for Regions B and C we get additional delta distribution terms in the variable z . Hence after evaluating the Q^2 integral with the optical theorem (2.22), we can re-sort these contributions according to

$$\frac{d\Gamma_A}{dz} = \frac{d\Gamma_A^{(0)}}{dz} \theta(1+z)\theta(1-z) \quad (2.49a)$$

$$\frac{d\Gamma_B}{dz} = \frac{d\Gamma_B^{(0)}}{dz} \theta(1+z)\theta(z_{\text{cut}} - z) + \sum_{n=1}^5 \frac{d\Gamma_B^{(n)}}{dz} \delta^{(n-1)}(z_{\text{cut}} - z) \quad (2.49b)$$

$$\frac{d\Gamma_C}{dz} = \frac{d\Gamma_C^{(0)}}{dz} \theta(-z_{\text{cut}} + z)\theta(1-z) + \sum_{n=1}^5 \frac{d\Gamma_C^{(n)}}{dz} \delta^{(n-1)}(z_{\text{cut}} - z) . \quad (2.49c)$$

We obtain the complete differential rate with

$$\frac{d\Gamma}{dz} = \frac{d\Gamma_A}{dz} + \frac{d\Gamma_B}{dz} + \frac{d\Gamma_C}{dz} . \quad (2.50)$$

³For the precision of theoretical predictions a lower cut would be preferred, as a too large cut has an impact on the validity of the HQE.

The integration to the forward-backward asymmetry or the total rate with the help of Eq. (2.32) and Eq. (2.33), respectively is now straight-forward. The $d\Gamma^{(0)}$ pieces need to be integrated with respect to z in their given limits, while higher order contributions are fixed by the delta distribution, which we need to treat as usual. Once again, we have checked our result for the total rate including the cut with previously calculated results using a different method. For the A_{FB} presented below we need to remember, that we have imposed the condition $z_{\text{cut}} \geq 0$. The cut will produce a non-smooth behaviour at the position of the cut, which we will investigate later. The discussion about the use of moments in the angular variables z is similar to Eq. (2.35), however obstructed due to the cut, which will shift contributions. We will not investigate this further.

3 Comparison of Expressions to Order $1/m_b^3$

First we will examine the analytic expressions from the known observables and the forward-backward asymmetry up to $\mathcal{O}(1/m_b^3)$ in the HQE. For an easier comparison of the analytic structure, we expand each result in $\rho = m_c^2/m_b^2$ to order $\mathcal{O}(\rho^2)$. The full results are given in Appendix A. The total rate to this order is then given by

$$\begin{aligned} \Gamma = \frac{G_F^2 |V_{cb}|^2}{192\pi^3 m_b^5} & \left[(1 - 8\rho - 12\rho^2 \log \rho) \left(1 - \frac{\mu_\pi^2}{2m_b^2} \right) - \frac{\mu_G^2}{2m_b^2} (3 - 8\rho + 12\rho^2 \log \rho + 24\rho^2) \right. \\ & + \frac{\rho_D^3}{6m_b^3} (77 + 48 \log(\rho) - 88\rho + 36\rho^2 \log \rho + 24\rho^2) \\ & \left. + \frac{\rho_{LS}^3}{2m_b^3} (3 - 8\rho + 12\rho^2 \log \rho + 24\rho^2) \right]. \end{aligned} \quad (3.1)$$

The moments and forward-backward asymmetry are normalised to the total rate. As we are interested in the dependence on the heavy quark parameters for the fit, we expand the results in $1/m_b$. Note that starting at order $1/m_b^4$ we encounter mixed terms in this approach, e.g. we have $(\mu_\pi^2)^2$, but to the order we are considering the results, this does not occur. Thus any observable we are considering below, can be viewed as an expansion of a function given by

$$F = \frac{\sum_{i=0} n[i] \frac{1}{m_b^i}}{\sum_{j=0} d[j] \frac{1}{m_b^j}} \quad (3.2a)$$

$$\Rightarrow F_{\text{exp.}} = \frac{n[0]}{d[0]} + \frac{d[0]n[2] - d[2]n[0]}{d[0]^2 m_b^2} + \frac{d[0]n[3] - d[3]n[0]}{d[0]^2 m_b^3}. \quad (3.2b)$$

We have explicitly used the fact, that $1/m_b$ corrections vanish, hence $n[1] = d[1] = 0$. The denominator function $d[i]$ is always given by the total rate (A.1), while we list the numerator functions $n[i]$ in Eq. (A.2-A.4). We find for the forward-backward asymmetry,

where we have expanded the result both in ρ and $1/m_b$ for comparison

$$\begin{aligned}
A_{FB} = & \frac{1}{4} \left[1 - 12\rho + 12\rho^2 \log \rho + 64\rho^{3/2} - 186\rho^2 \right] \\
& + \frac{4\mu_\pi^2}{3m_b^2} \left[-1 + 6\sqrt{\rho} - 23\rho - 12\rho^2 \log \rho + 68\rho^{3/2} - 199\rho^2 \right] \\
& + \frac{\mu_G^2}{3m_b^2} \left[-4 + 24\sqrt{\rho} - 92\rho - 48\rho^2 \log \rho + 272\rho^{3/2} - 796\rho^2 \right] \\
& + \frac{\rho_D^3}{3m_b^3} \left[-14 - 6 \log \rho + 24\rho \log \rho + 16\sqrt{\rho} - 3\rho + 1020\rho^2 \log \rho - 144\rho^2 \log^2 \rho \right. \\
& \quad \left. + 1640\rho^2 - 384\rho^{3/2} \log \rho - 488\rho^{3/2} \right] + \frac{\rho_{LS}^3}{m_b^3} \left[-1 - 18\rho^2 \log \rho - 24\rho^{3/2} + 51\rho^2 \right].
\end{aligned} \tag{3.3}$$

We see, that especially for the lowest order, there is a similar dependence as for the normalisation and hence the $|V_{cb}|$ extraction. The HQE parameters themselves are extracted from moments, currently the charged lepton energy and hadronic invariant mass one. We quote the most important moments [29] in the same way as we have done for the forward-backward asymmetry. The charged lepton energy moment is given by

$$\begin{aligned}
\langle E_\ell \rangle = & \frac{m_b}{20} \left[1 + \frac{\mu_\pi^2}{2m_b^2} \right] [7 - 19\rho + 96\rho^2 \log \rho - 272\rho^2] \\
& - \frac{\mu_G^2}{120m_b} [7288\rho^2 + 695\rho + 48(67\rho + 5)\rho \log \rho + 57] \\
& + \frac{\rho_D^3}{360m_b^2} [128744\rho^2 + 19008\rho^2 \log^2 \rho + 48(2384\rho^2 + 109\rho + 9) \log \rho + 8389\rho + 999] \\
& + \frac{\rho_{LS}^3}{40m_b^2} [872\rho^2 + 240\rho^2 \log \rho + 17\rho + 3].
\end{aligned} \tag{3.4}$$

The partonic invariant mass and energy are related to the hadronic invariant mass by

$$M_X^2 = (P_B - q)^2 = M_B^2 - 2M_B v \cdot q + q^2 \tag{3.5}$$

and hence we need to introduce the dependence to the mass of the B -meson. It is obvious to identify the source of each of the terms below from that equation

$$\begin{aligned}
\langle M_X^2 \rangle = & M_B^2 + m_b M_B \left(\frac{204\rho^2}{5} + \frac{72}{5}\rho^2 \log \rho + \frac{31\rho}{10} - \frac{13}{10} \right) \\
& + m_b^2 \left(-\frac{204\rho^2}{5} - \frac{72}{5}\rho^2 \log \rho - \frac{21\rho}{10} + \frac{3}{10} \right) \\
& + \frac{\mu_\pi^2}{m_b^2} \left[m_b M_B \left(\frac{102\rho^2}{5} + \frac{36}{5}\rho^2 \log \rho + \frac{31\rho}{20} - \frac{13}{20} \right) \right] \\
& + \frac{\mu_G^2}{m_b^2} \left[m_b M_B \left(\frac{756\rho^2}{5} + \frac{312}{5}\rho^2 \log \rho + \frac{151\rho}{12} + 4\rho \log \rho + \frac{21}{20} \right) \right. \\
& \left. + m_b^2 \left(-\frac{2098\rho^2}{15} - \frac{292}{5}\rho^2 \log \rho - \frac{34\rho}{3} - 4\rho \log \rho - \frac{4}{5} \right) \right] \\
& + \frac{\rho_D^3}{m_b^3} m_b^2 \left[\frac{82}{5} + \frac{5026\rho}{45} + \frac{12790\rho^2}{9} + \frac{964}{15}\rho \log(\rho) + \frac{28 \log \rho}{5} \right. \\
& \left. + \frac{912}{5}\rho^2 \log^2 \rho + \frac{3592}{3}\rho^2 \log \rho \right] \\
& + \frac{\rho_{LS}^3}{m_b^3} \left[m_b^2 \left(\frac{2098\rho^2}{15} + \frac{292}{5}\rho^2 \log \rho + \frac{34\rho}{3} + 4\rho \log \rho + \frac{4}{5} \right) \right]. \tag{3.6}
\end{aligned}$$

For an easier comparison of the functional form of the expanded results, we quote the dependence numerically using the numerical result from [18] with $\rho \approx 0.047$. Here we have only expanded in $1/m_b$ and keep the full dependence on ρ

$$\Gamma \approx 0.706 - \frac{0.353\mu_\pi^2}{m_b^2} - \frac{1.297\mu_G^2}{m_b^2} - \frac{12.350\rho_D^3}{m_b^3} + \frac{1.297\rho_{LS}^3}{m_b^3} \tag{3.7}$$

$$A_{FB} \approx 0.135 - \frac{0.376\mu_\pi^2}{m_b^2} - \frac{1.197\mu_G^2}{m_b^2} - \frac{0.570\rho_D^3}{m_b^3} - \frac{0.516\rho_{LS}^3}{m_b^3} \tag{3.8}$$

$$\langle E_\ell \rangle \approx m_b \left[0.316 + \frac{0.158\mu_\pi^2}{m_b^2} - \frac{0.379\mu_G^2}{m_b^2} - \frac{1.999\rho_D^3}{m_b^3} + \frac{0.087\rho_{LS}^3}{m_b^3} \right] \tag{3.9}$$

$$\begin{aligned}
\langle m_X^2 \rangle \approx & \frac{1}{m_b} \left[M_B^2 m_b - 1.187 M_B m_b^2 + 0.234 m_b^3 - 0.594 \mu_\pi^2 M_B \right. \\
& \left. + \mu_G^2 (0.890 M_B - 0.590 m_b) - 5.471 \rho_D^3 + 0.590 \rho_{LS}^3 \right]. \tag{3.10}
\end{aligned}$$

From this, we can see that the coefficients of μ_π^2 and μ_G^2 have opposite signs for the moments, while same sign coefficients for the rate and the forward-backward asymmetry. It has been known before, that the sensitivity to μ_G^2 and ρ_{LS}^3 is low for all currently used observables. The sensitivity to μ_G^2 is enhanced for A_{FB} and therefore we gain useful information. Furthermore the higher order contributions seem to be stronger suppressed for the A_{FB} . Hence we are able to extract a further linear combination, which is especially useful for the normalisation. In that sense, the value of μ_G^2 seems to be stronger constraint.

4 Numerical Results to Order $1/m_b^5$

First we investigate the differential spectrum in $z = \cos\theta$ itself. On the left-hand side in Fig. 2 we have displayed the spectrum itself with no minimum energy cut on the charged lepton. The individual colour coded curves are contributions including $1/m_b^n$ corrections to the order: $1/m_b^0$ (black), $1/m_b^2$ (green), $1/m_b^3$ (red dashed), $1/m_b^4$ (orange long-dashed) and $1/m_b^5$ (blue dotted).

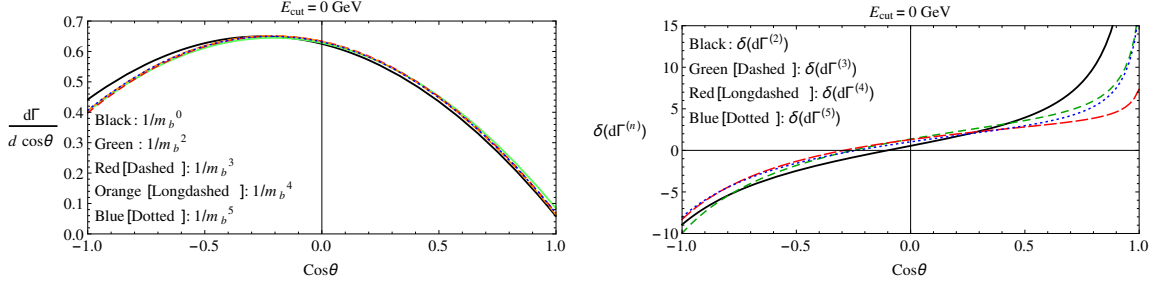


Figure 2. The differential rate $\frac{d\Gamma}{d \cos\theta}$ as a function of the angle $z = \cos\theta$ with no energy cut on the charged lepton. Left: The spectrum itself for various orders in $1/m_b$. Right: Relative contribution $\delta = 100 \frac{d\Gamma^{(n)} - d\Gamma^{(3)}}{d\Gamma^{(3)}}$ from order $1/m_b^n$ to the partonic rate.

We find, that the corrections are getting larger for approaching the physical endpoints of the angle. As the rate is approaching zero for $z = \cos\theta \rightarrow 1$, the absolute deviations are hardly visible in the left plot, while the corrections for $z \rightarrow -1$ are larger in absolute values and hence visible in the plot, although the relative corrections are smaller. Roughly, the corrections for negative z are negative, while for positive z they are positive. These interesting facts seem to be related to the kinematics of the final state charm system, which is sensitive to heavy quark corrections. The corrections themselves are in reasonable size and behave as expected for higher-orders. For this remember, that the hadronic tensor depends on $v \cdot q$ and q^2 , while z is a function of $v \cdot q$ and q^2 , as well as the charged electron energy.

From the left plot, we can see the asymmetric behaviour of the spectrum, and hence a forward-backward asymmetry can be observed. Especially we find for higher-order corrections, that the $1/m_b^2$ corrections are very important. The convergence of higher order terms in the expansion is good and stable. Hence in combination with the fact, that we are sensitive to a particular combination of μ_π^2 and especially μ_G^2 , see Eqs. (3.3) and (3.8), from this observable we have a good sensitivity to μ_G^2 .

In real experimental environments, we have to impose a minimum cut on the charged lepton energy. In the following we investigate the consequences on the differential spectrum. A realistic cut from current experiments is $E_{\text{cut}} = 1$ GeV [18], while the hope is to reduce this in future experiments to even lower values. It is well-known that restricting the phase-space limits the validity of the heavy quark expansion and hence higher-order terms have a larger impact. Currently it is estimated, that the HQE works still to a reasonable precision for $E_{\text{cut}} \lesssim 1.5$ GeV [29], but $E_{\text{cut}} \approx 1$ GeV is certainly preferred.

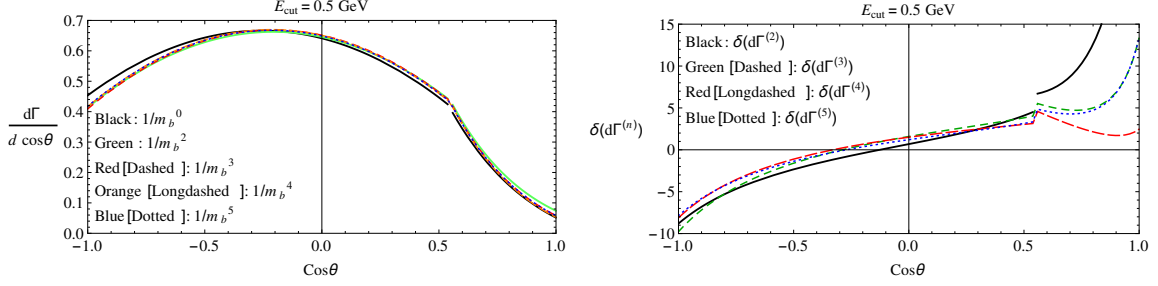


Figure 3. The differential rate $\frac{d\Gamma}{d \cos\theta}$ as a function of the angle $z = \cos\theta$ with a minimum energy cut on the charged lepton of $E_{\text{cut}} = 0.5 \text{ GeV}$. Left: The spectrum itself for various orders in $1/m_b$, right relative contribution $\delta = 100 \frac{d\Gamma^{(n)} - d\Gamma^{(3)}}{d\Gamma^{(3)}}$ from order $1/m_b^n$ to the partonic rate.

In Fig. 3 we compare the same plots as before, now imposing a cut of $E_{\text{cut}} = 0.5 \text{ GeV}$. In this scenario, we observe a kink in the theoretical spectrum exactly at the cut separation

$$z_{\text{cut}} = 1 - \frac{4E_{\text{cut}}m_b}{m_b^2 - m_c^2}. \quad (4.1)$$

We find, that for the partonic rate the spectrum behaves unsteady at this position. For higher-orders this becomes worse and we find a discontinuity. This exactly reflects the fact, that we are expanding a non-local object into local terms. In reality this kink will be smoothed out by the distribution of the final state mass.

As obvious from Figs. 4 and 5, the latter has a cut of $E_{\text{cut}} = 1 \text{ GeV}$ used in current data, the cut moves to smaller values of z and the discontinuity is enhanced. While the relative corrections in the right side plot are stable for $z < z_{\text{cut}}$ they are getting larger for $z > z_{\text{cut}}$ and the hierarchy of corrections to various orders is clearly visible. Interestingly the effect of $\mathcal{O}(1/m_b^4)$ seems to be stronger, while $\mathcal{O}(1/m_b^5)$ approaches $\mathcal{O}(1/m_b^3)$ and both of the latter seem to be more stable for $z \rightarrow 1$. Please note, that the spectrum is shifted towards the negative values of z with increasing cut.

For the maximal cut of $E_{\text{cut}}^{\text{max}} = \frac{m_b^2 - m_c^2}{4m_b}$ we find in Fig. 6, that the separation is exactly

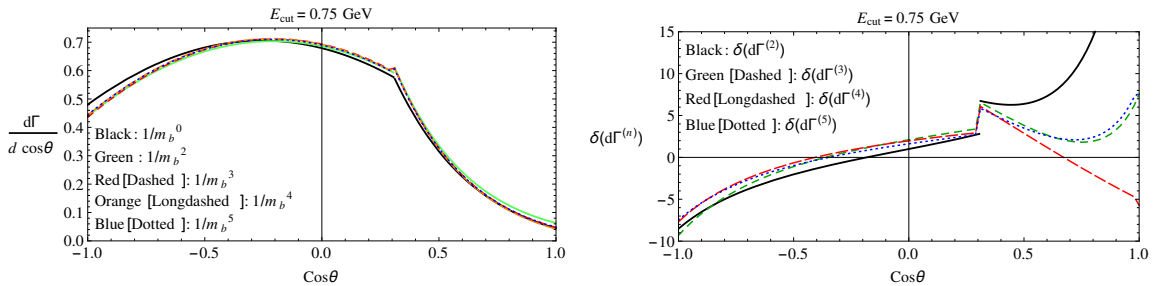


Figure 4. The differential rate $\frac{d\Gamma}{d \cos\theta}$ as a function of the angle $z = \cos\theta$ with a minimum energy cut on the charged lepton of $E_{\text{cut}} = 0.75 \text{ GeV}$. Left: The spectrum itself for various orders in $1/m_b$, right relative contribution $\delta = 100 \frac{d\Gamma^{(n)} - d\Gamma^{(3)}}{d\Gamma^{(3)}}$ from order $1/m_b^n$ to the partonic rate.

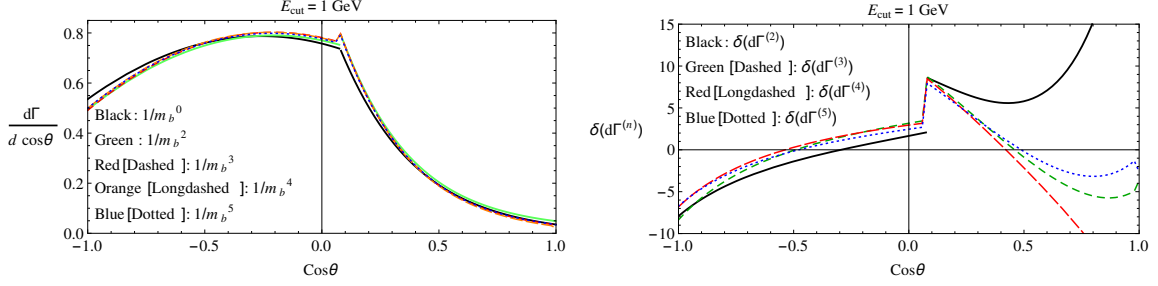


Figure 5. The differential rate $\frac{d\Gamma}{d \cos\theta}$ as a function of the angle $z = \cos\theta$ with a minimum energy cut on the charged lepton of $E_{\text{cut}} = 1$ GeV. Left: The spectrum itself for various orders in $1/m_b$, right relative contribution $\delta = 100 \frac{d\Gamma^{(n)} - d\Gamma^{(3)}}{d\Gamma^{(3)}}$ from order $1/m_b^n$ to the partonic rate.

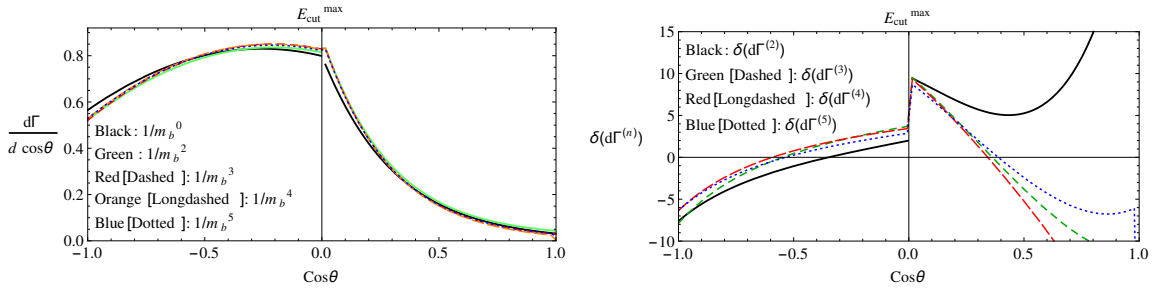


Figure 6. The differential rate $\frac{d\Gamma}{d \cos\theta}$ as a function of the angle $z = \cos\theta$ with a maximal energy cut on the charged lepton of $E_{\text{cut}} = \frac{m_b^2 - m_c^2}{4m_b} \approx 1.08$ GeV, such that the cut separation is still positive. Left: The spectrum itself for various orders in $1/m_b$, right relative contribution $\delta = 100 \frac{d\Gamma^{(n)} - d\Gamma^{(3)}}{d\Gamma^{(3)}}$ from order $1/m_b^n$ to the partonic rate.

at $z = 0$, which was our definition for the maximal allowed cut in this scenario. Of course theoretically the cut may even be larger, but then our predictions for the A_{FB} would have to be modified, as terms shift from positive to negative. As stated before on the one hand this maximal cut is above the current experimentally used cuts, and on the other hand the larger the cut the less precise are our predictions and hence our restriction.

In general, only fully integrated observables over the hadronic kinematics are investigated [29], with the only exception of the distribution in the charged lepton energy. The heavy-quark spin-symmetry is only valid for fully integrated observables over the hadronic part, as it starts from a spherical symmetry. The charged lepton energy is (mainly) independent from the hadronic kinematics and hence can be utilised as an additional observable. Here we find this feature, that z strongly depends on the hadronic kinematics, which is reflect by this unsteady behaviour.

For this particular observable we find, that the correction seem to play a more important role for $z \rightarrow 1$. That indicates the relation to the final state kinematics of the hadron system. In exclusive transitions HQE works fine, if the final and initial state hadron is moving with the same velocity, while it breaks down for a vastly different situation. That

effect seems to be resembled in this particular spectrum, although we are investigating a property of the leptonic system, its kinematics is connected to the hadron system.

We will comment more on the situation and use of this spectrum in Sec. 5, and turn now to the integrated forward-backward asymmetry A_{FB} .

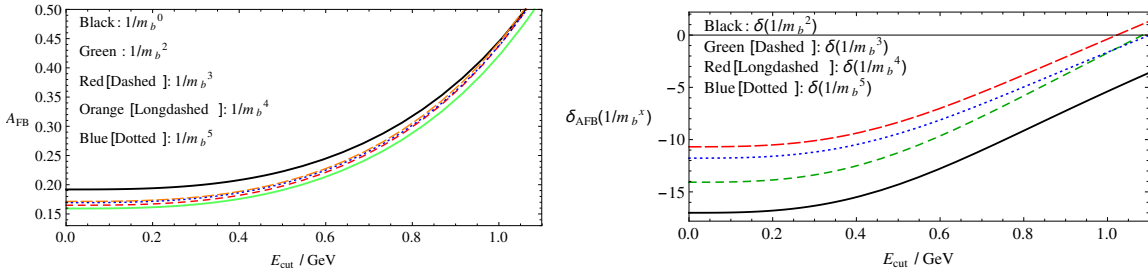


Figure 7. The forward-backward asymmetry A_{FB} as a function of the minimal energy cut on the charged lepton. Left: A_{FB} for various orders in $1/m_b$, right relative contribution $\delta = 100 \frac{A_{FB}^{(n)} - A_{FB}^{(3)}}{A_{FB}^{(3)}}$ from order $1/m_b^n$ to the partonic contribution.

We have plotted the forward-backward asymmetry A_{FB} in Fig. 7 as a function of the cut in the left plot. The colour coding is: contributions included up to $1/m_b^0$ (black), $1/m_b^2$ (green), $1/m_b^3$ (red dashed), $1/m_b^4$ (orange long-dashed) and $1/m_b^5$ (blue dotted). In the same way as before, we plot the relative correction

$$\delta = 100 \frac{A_{FB}^{(n)} - A_{FB}^{(3)}}{A_{FB}^{(3)}} \quad (4.2)$$

on the right hand side of the figure. The corrections of $1/m_b^2$ are by far the biggest one, and hence we are sensitive to them. As obvious from the spectrum, for a larger cut on the charged lepton energy, we find an increasing A_{FB} . The relative corrections are, contrary to naive expectations, decreasing for a higher cut. That effect is most probably driven by the fact, that the A_{FB} increases for larger E_{cut} , and the partonic contribution is growing obviously faster. Even though we have an increasing forward-backward asymmetry with larger cuts, the absolute difference of the higher order terms is larger for a smaller cut. The effect of including higher order is as expected getting smaller, however again we find that the pure $1/m_b^5$ corrections have the opposite sign, as can be seen from the right plot in Fig. 7.

We may now investigate the stability of this sensitivity to the $1/m_b^2$ parameters while including higher-order terms along the line of [29]. Defining an observable as $\mathcal{M}^{(n)}$, where n denotes the order in $1/m_b^n$, we can assess the effect to a single heavy-quark parameter (HQP) with including higher-order terms by

$$\delta\text{HQP} = - \frac{\mathcal{M}^{(5)} - \mathcal{M}^{(3)}}{\frac{\partial \mathcal{M}^{(3)}}{\partial \text{HQP}}}. \quad (4.3)$$

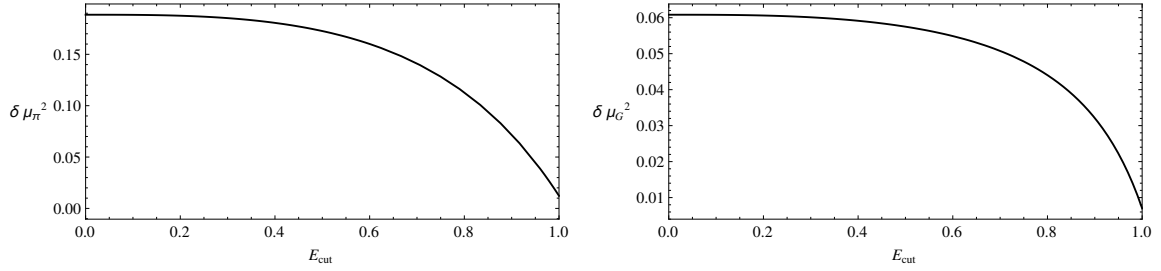


Figure 8. Estimating the effect on μ_π^2 and μ_G^2 of including $1/m_b^{4,5}$ in the forward-backward asymmetry using Eq. (4.3) as a function of E_{cut} .

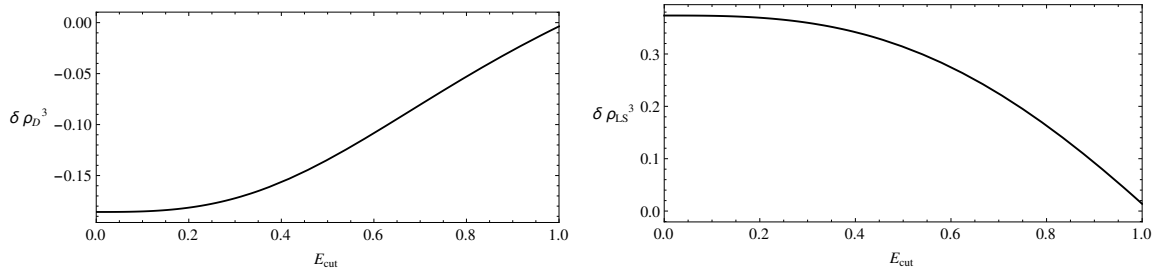


Figure 9. Estimating the effect on ρ_D^3 and ρ_{LS}^3 of including $1/m_b^{4,5}$ in the forward-backward asymmetry using Eq. (4.3) as a function of E_{cut} .

The results for \mathcal{M} being the forward-backward asymmetry A_{FB} for the two parameters in $1/m_b^2$ are plotted in Fig. 8, while the effect on the two parameters in $1/m_b^3$ are plotted in Fig. 9 as a function of the minimum charged lepton energy cut.

We find, that for increasing cut the effect for each of the non-perturbative parameters is getting very small. The situation for a small cut, however, is different. We would deem the effects on μ_π^2 , ρ_D^3 and especially on ρ_{LS}^3 as significant, and too large. This indicates, that we are not in particular sensitive to those heavy quark parameters. The situation for μ_G^2 is a bit different. Here the shift is in a reasonable order of magnitude and the effect with a large energy cut is the largest, while the dependence on the charged lepton energy cut is the smallest. This more stable situation confirms our previous finding, that we are most sensitive to μ_G^2 . It also reflects the fact, that higher-order terms are getting less important for an increasing cut on the charged lepton energy, which is contrary to naive expectations.

5 Discussion

We have investigated inclusive semi-leptonic $B \rightarrow X_c \ell \bar{\nu}_\ell$ decays in the context of heavy quark expansion, especially with focus on a new observable. Our proposal is to utilise the forward-backward asymmetry of the charged lepton as an additional constraint in measurements to obtain information about the heavy quark parameters.

First we have derived the triple differential decay rate in Eq. (2.16) including phase-space effects due to a minimum energy cut on the charged lepton energy, which is required

experimentally. After revisiting the specific application of the heavy quark expansion in this case, we construct the observable.

In section 3, we have analysed the properties of the forward-backward asymmetry without a cut at lower orders and compared to the already existing observables, i.e. moments of the hadronic invariant mass and charged lepton energy. It turns out, that we are specifically sensitive to the $1/m_b^2$ corrections, and the linear combination of μ_π^2 and μ_G^2 is very similar to the total rate, from which $|V_{cb}|$ is finally extracted. Hence we expect a large sensitivity to the chromo-magnetic moment μ_G^2 , which can currently not be constrained very well from experimental analysis in this decay mode.

Following up, we have investigated the full corrections in section 4, numerically. First we had a closer look onto the differential spectrum in $z = \cos\theta$. It turns out, that in this spectrum a cut on the charged lepton energy induces a discontinuity, that is related to the hadronic system. This discontinuity is smoothed out by a finite mass distribution of the hadronic system in reality. As this fact reflects the dependence on the hadronic system in this variable, it is not advisable to use this spectrum as an observable. However, integrated rates do not suffer from this issue.

We therefore have analysed the forward-backward asymmetry A_{FB} . As said, it is sensitive to the $1/m_b^2$ corrections, and especially it seems, that μ_G^2 may be constraint reasonably well from this for the first time only due to this decay analysis. It is a good candidate for an additional observable, that will help to validate the heavy quark expansion, and at the same time increase the precision on the extraction of $|V_{cb}|$.

In the numerical analysis it turns out, that the $1/m_b^4$ corrections seem to be particularly large, while the corrections including $1/m_b^5$ are stable and approach the results known from $1/m_b^3$ more closely. That might be related to the occurrence of intrinsic charm operators, that mix the different orders in power-counting starting at $1/m_b^4$ [32].

In future, one can study if New Physics operators, e.g. right-handed currents, have a larger impact on this observable and hence may be constraint in a better way.

Furthermore one could in principle study a combined charged electron energy and/or hadronic invariant mass moment and A_{FB} analysis, provided that this is experimentally feasible. For a generic observable, which combines A_{FB} and a moment in the kinematic variable \mathcal{M} we define

$$\langle \mathcal{M} \rangle_{A_{FB}} = \frac{\int_{-1}^0 dz \int d\mathcal{M} \frac{d^2\Gamma}{dz d\mathcal{M}} \mathcal{M} - \int_0^1 dz \int d\mathcal{M} \frac{d^2\Gamma}{dz d\mathcal{M}} \mathcal{M}}{\int_{-1}^1 dz \int d\mathcal{M} \frac{d^2\Gamma}{dz d\mathcal{M}}}. \quad (5.1)$$

This combination induces of course correlations with the other observables, but it may be sensitive to higher dimensional HQE parameters, which are not accessible right now. Evaluating this observable from Eq. (2.13), this corresponds to moments of the hadronic structure function W_3 , which again are not taken into account in current analysis. For the predictions of the charged lepton energy moment $\langle E_\ell \rangle_{A_{FB}}$ combined with the forward-backward asymmetry, one needs to weight the integral over the triple differential rate with a factor of

$$\mathcal{M} = E_\ell = \frac{1}{2}(v \cdot q - z \sqrt{v \cdot q^2 - q^2}) = \frac{1}{2}(m_b - v \cdot Q - z \sqrt{v \cdot Q^2 - Q^2}), \quad (5.2)$$

see Eq. (2.14), while for the hadronic invariant mass $\langle M_X^2 \rangle_{AFB}$ moment, we need the proper linear combination of moments in $v \cdot q$ and q^2

$$\mathcal{M} = M_X^2 = M_B^2 - 2M_B v \cdot q + q^2 = (M_B - m_b)^2 + 2(M_B - m_b)v \cdot Q + Q^2. \quad (5.3)$$

As higher orders in M_X^2 are in particular sensitive to $1/m_b$ correction terms in the expansion, see Eq. (2.22), we expect that the first moment in M_X^2 for the A_{FB} potentially has an enlarged sensitivity to ρ_{LS}^3 , see the discussion around Fig. 8 and 9.

The achievable experimental uncertainties depend very much on the precision of the neutrino momentum reconstruction. For inclusive analysis, where the hadronic final state is not specified, this is obviously worse than for exclusive final states. However as we are interested in the normalised forward-backward asymmetry, only, and not in the angular spectrum, hopefully most of the systematic uncertainties drop out. A remaining issue will probably be the migration of reconstructed events around the separations, i.e. $z = 0$ and $z = z_{\text{cut}}$. A careful experimental analysis is required in order to assess an achievable precision for these observables.

In summary we have proposed a new observable for the analysis of semi-leptonic $B \rightarrow X_c \ell \bar{\nu}_\ell$ decays. We have shown, that this observable is indeed useful and have calculated the non-perturbative corrections up to $\mathcal{O}(1/m_b^5)$.

Acknowledgments

S.T. is supported by the ERC Advanced Grant EFT4LHC of the European Research Council and the Cluster of Excellence Precision Physics, Fundamental Interactions and Structure of Matter (PRISMA-EXC 1098). S.T. is grateful to Florian Bernlochner for useful discussions and comments about this manuscript. The author would like to express special thanks to the Mainz Institute for Theoretical Physics (MITP) for its hospitality and support during the workshop "Challenges in Semileptonic B decays", where part of this work has been developed and discussed.

A Full Analytic Results to Order $\mathcal{O}(1/m_b^3)$

The total rate is given by

$$\begin{aligned} \Gamma = & \frac{G_F^2 |V_{cb}|^2}{192\pi^3 m_b^5} \left[1 - 8\rho - 12\rho^2 \log \rho + 8\rho^3 - \rho^4 \right. \\ & - \frac{\mu_\pi^2}{2m_b^2} \left(1 - 8\rho - 12\rho^2 \log \rho + 8\rho^3 - \rho^4 \right) \\ & + \frac{\mu_G^2}{2m_b^2} \left(-3 + 8\rho - 12\rho^2 \log \rho - 24\rho^2 + 24\rho^3 - 5\rho^4 \right) \\ & + \frac{\rho_D^3}{6m_b^3} \left(77 + 48 \log(\rho) - 88\rho + 36\rho^2 \log \rho + 24\rho^2 - 8\rho^3 - 5\rho^4 \right) \\ & \left. - \frac{\rho_{LS}^3}{2m_b^3} \left(-3 + 8\rho - 12\rho^2 \log \rho - 24\rho^2 + 24\rho^3 - 5\rho^4 \right) + \mathcal{O}\left(\frac{1}{m_b^4}\right) \right]. \quad (\text{A.1}) \end{aligned}$$

The forward-backward asymmetry is given by

$$\begin{aligned}
\Gamma \cdot A_{FB} = & \frac{1}{4} \left(1 - 20\rho - 90\rho^2 - 20\rho^3 + \rho^4 + 64\rho^{3/2} + 64\rho^{5/2} \right) \\
& - \frac{\mu_\pi^2}{24m_b^2} \left(35 - 192\sqrt{\rho} + 420\rho + 210\rho^2 - 28\rho^3 + 3\rho^4 - 448\rho^{3/2} \right) \\
& + \frac{\mu_G^2}{24m_b^2} \left(-65 + 192\sqrt{\rho} - 60\rho + 330\rho^2 - 92\rho^3 + 15\rho^4 - 320\rho^{3/2} \right) \\
& + \frac{\rho_D^3}{24m_b^3} \left(-35 + 128\sqrt{\rho} - 140\rho + 70\rho^2 - 28\rho^3 + 5\rho^4 \right) \\
& - \frac{\rho_{LS}^3}{8m_b^3} \left(5 - 20\rho + 30\rho^2 - 20\rho^3 + 5\rho^4 \right) + \mathcal{O}\left(\frac{1}{m_b^4}\right). \tag{A.2}
\end{aligned}$$

The first charged lepton energy moment is given by

$$\begin{aligned}
\Gamma \cdot \langle E_\ell \rangle = & \frac{m_b}{20} \left(3\rho^5 - 15\rho^4 + 200\rho^3 - 60\rho^3 \log \rho - 120\rho^2 - 180\rho^2 \log \rho - 75\rho + 7 \right) \\
& + \frac{\mu_G^2}{6m_b} \left(3\rho^5 - 14\rho^4 + 24\rho^3 - 12\rho^2 + 5\rho - 12\rho \log \rho - 6 \right) \\
& + \frac{\rho_D^3}{45m_b^2} \left(18\rho^5 - 35\rho^4 - 120\rho^3 + 540\rho^2 - 730\rho - 120\rho \log \rho + 180 \log \rho + 327 \right) \\
& - \frac{3\rho_{LS}^3}{5m_b^2} \left(-\rho^5 + 5\rho^4 - 10\rho^3 + 10\rho^2 - 5\rho + 1 \right) + \mathcal{O}\left(\frac{1}{m_b^4}\right). \tag{A.3}
\end{aligned}$$

The first hadronic invariant mass moment is given by

$$\begin{aligned}
\Gamma \cdot \langle M_X^2 \rangle = & m_b M_B \left(-\frac{7\rho^5}{10} + \frac{9\rho^4}{2} - 32\rho^3 + 6\rho^3 \log \rho + 16\rho^2 + 30\rho^2 \log \rho + \frac{27\rho}{2} - \frac{13}{10} \right) \\
& + m_b^2 \left(-\frac{3\rho^5}{10} + \frac{9\rho^4}{2} + 24\rho^3 - 18\rho^3 \log \rho - 24\rho^2 - 18\rho^2 \log \rho - \frac{9\rho}{2} + \frac{3}{10} \right) \\
& + M_B^2 (-\rho^4 + 8\rho^3 - 12\rho^2 \log \rho - 8\rho + 1) \\
& + \frac{\mu_\pi^2}{m_b^2} \left[m_b^2 \left(\frac{3\rho^5}{20} - \frac{9\rho^4}{4} - 12\rho^3 + 9\rho^3 \log \rho + 12\rho^2 + 9\rho^2 \log \rho + \frac{9\rho}{4} - \frac{3}{20} \right) \right] \\
& + M_B^2 \left(\frac{\rho^4}{2} - 4\rho^3 + 6\rho^2 \log \rho + 4\rho - \frac{1}{2} \right) \\
& + \frac{\mu_G^2}{m_b^2} \left[m_b M_B \left(3 - \frac{7\rho^5}{3} + \frac{35\rho^4}{3} - 24\rho^3 + \frac{52\rho^2}{3} + 4\rho^2 \log \rho - \frac{17\rho}{3} + 4\rho \log \rho \right) \right. \\
& + m_b^2 \left(-\frac{3\rho^5}{4} + \frac{79\rho^4}{12} - 4\rho^3 - 9\rho^3 \log \rho + 3\rho^2 \log \rho - \frac{7\rho}{12} - 4\rho \log(\rho) - \frac{5}{4} \right) \\
& \left. + M_B^2 \left(-\frac{5\rho^4}{2} + 12\rho^3 - 12\rho^2 - 6\rho^2 \log \rho + 4\rho - \frac{3}{2} \right) \right] \\
& + \frac{\rho_D^3}{m_b^3} \left[M_B^2 \left(-\frac{5\rho^4}{6} - \frac{4\rho^3}{3} + 4\rho^2 + 6\rho^2 \log \rho - \frac{44\rho}{3} + 8 \log \rho + \frac{77}{6} \right) \right. \\
& + m_b M_B \left(-\frac{28\rho^5}{15} + \frac{44\rho^4}{9} + \frac{16\rho^3}{3} - \frac{112\rho^2}{3} + \frac{532\rho}{9} + \frac{16}{3} \rho \log \rho - 16 \log \rho - \frac{452}{15} \right) \\
& + m_b^2 \left(-\frac{\rho^5}{4} - \frac{41\rho^4}{36} - 4\rho^3 + 9\rho^3 \log \rho + 36\rho^2 - 23\rho^2 \log \rho \right. \\
& \left. - \frac{1831\rho}{36} + \frac{8}{3} \rho \log \rho + 8 \log \rho + \frac{81}{4} \right) \left. \right] \\
& + \frac{\rho_{LS}^3}{m_b^3} \left[\left(\frac{14\rho^5}{5} - 14\rho^4 + 28\rho^3 - 28\rho^2 + 14\rho - \frac{14}{5} \right) m_b M_B \right. \\
& + m_b^2 \left(\frac{3\rho^5}{4} - \frac{79\rho^4}{12} + 4\rho^3 + 9\rho^3 \log \rho - 3\rho^2 \log \rho + \frac{7\rho}{12} + 4\rho \log \rho + \frac{5}{4} \right) \\
& \left. + M_B^2 \left(\frac{5\rho^4}{2} - 12\rho^3 + 12\rho^2 + 6\rho^2 \log \rho - 4\rho + \frac{3}{2} \right) \right] + \mathcal{O}\left(\frac{1}{m_b^4}\right). \tag{A.4}
\end{aligned}$$

References

- [1] K. A. Olive *et al.* [Particle Data Group Collaboration], *Chin. Phys. C* **38** (2014) 090001.
- [2] J. Chay, H. Georgi and B. Grinstein, *Phys. Lett. B* **247**, 399 (1990).
- [3] I. I. Y. Bigi, M. A. Shifman, N. G. Uraltsev and A. I. Vainshtein, *Phys. Rev. Lett.* **71**, 496 (1993) [arXiv:hep-ph/9304225].
- [4] A. V. Manohar and M. B. Wise, *Phys. Rev. D* **49**, 1310 (1994) [arXiv:hep-ph/9308246].
- [5] T. Mannel, *Nucl. Phys. B* **413**, 396 (1994) [arXiv:hep-ph/9308262].
- [6] B. Aubert *et al.* [BaBar Collaboration], anti-B \rightarrow j X(c) l- anti-nu," *Phys. Rev. D* **81** (2010) 032003 [arXiv:0908.0415 [hep-ex]].

- [7] B. Aubert *et al.* [BaBar Collaboration], Phys. Rev. D **69** (2004) 111104 [hep-ex/0403030].
- [8] P. Urquijo *et al.* [Belle Collaboration], $B \rightarrow \bar{c} X(c) e \nu$ decays at Belle,” Phys. Rev. D **75** (2007) 032001 [hep-ex/0610012].
- [9] C. Schwanda *et al.* [Belle Collaboration], Decays at BELLE,” Phys. Rev. D **75** (2007) 032005 [hep-ex/0611044].
- [10] C. Schwanda *et al.* [Belle Collaboration], gamma Decays and Determination of $|V_{cb}|$ and $m(b)$ at Belle,” Phys. Rev. D **78** (2008) 032016 [arXiv:0803.2158 [hep-ex]].
- [11] D. Acosta *et al.* [CDF Collaboration], Phys. Rev. D **71** (2005) 051103 [hep-ex/0502003].
- [12] S. E. Csorna *et al.* [CLEO Collaboration], Phys. Rev. D **70** (2004) 032002 [hep-ex/0403052].
- [13] J. Abdallah *et al.* [DELPHI Collaboration], Eur. Phys. J. C **45** (2006) 35 [hep-ex/0510024].
- [14] D. Benson, I. I. Bigi, T. Mannel and N. Uraltsev, Nucl. Phys. B **665**, 367 (2003) [arXiv:hep-ph/0302262].
- [15] P. Gambino and N. Uraltsev, Eur. Phys. J. C **34**, 181 (2004) [arXiv:hep-ph/0401063].
- [16] C. W. Bauer, Z. Ligeti, M. Luke and A. V. Manohar, Phys. Rev. D **67**, 054012 (2003) [arXiv:hep-ph/0210027].
- [17] A. H. Hoang, Z. Ligeti and A. V. Manohar, Phys. Rev. D **59**, 074017 (1999) [arXiv:hep-ph/9811239].
- [18] A. Alberti, P. Gambino, K. J. Healey and S. Nandi, Phys. Rev. Lett. **114** (2015) 6, 061802 [arXiv:1411.6560 [hep-ph]].
- [19] K. Melnikov, Phys. Lett. B **666** (2008) 336 [arXiv:0803.0951 [hep-ph]].
- [20] A. Pak and A. Czarnecki, Phys. Rev. Lett. **100** (2008) 241807 [arXiv:0803.0960 [hep-ph]].
- [21] T. Becher, H. Boos and E. Lunghi, JHEP **0712** (2007) 062 [arXiv:0708.0855 [hep-ph]].
- [22] A. Alberti, T. Ewerth, P. Gambino and S. Nandi, Nucl. Phys. B **870** (2013) 16 [arXiv:1212.5082 [hep-ph]].
- [23] A. Alberti, P. Gambino and S. Nandi, JHEP **1401** (2014) 147 [arXiv:1311.7381 [hep-ph]].
- [24] T. Mannel, A. A. Pivovarov and D. Rosenthal, Phys. Lett. B **741** (2015) 290 [arXiv:1405.5072 [hep-ph]].
- [25] T. Mannel, A. A. Pivovarov and D. Rosenthal, Phys. Rev. D **92** (2015) 5, 054025 [arXiv:1506.08167 [hep-ph]].
- [26] B. Blok, L. Koyrakh, M. A. Shifman and A. I. Vainshtein, Phys. Rev. D **49** (1994) 3356 [Phys. Rev. D **50** (1994) 3572] [hep-ph/9307247].
- [27] M. Gremm and A. Kapustin, Phys. Rev. D **55** (1997) 6924 [hep-ph/9603448].
- [28] B. M. Dassinger, T. Mannel and S. Turczyk, JHEP **0703** (2007) 087 [hep-ph/0611168].
- [29] T. Mannel, S. Turczyk and N. Uraltsev, JHEP **1011** (2010) 109 [arXiv:1009.4622 [hep-ph]].
- [30] I. I. Bigi, N. Uraltsev and R. Zwicky, Eur. Phys. J. C **50** (2007) 539 [hep-ph/0511158].
- [31] C. Breidenbach, T. Feldmann, T. Mannel and S. Turczyk, Phys. Rev. D **78** (2008) 014022 [arXiv:0805.0971 [hep-ph]].
- [32] I. Bigi, T. Mannel, S. Turczyk and N. Uraltsev, JHEP **1004** (2010) 073 [arXiv:0911.3322 [hep-ph]].

- [33] C. W. Bauer, Z. Ligeti, M. Luke, A. V. Manohar and M. Trott, Phys. Rev. D **70** (2004) 094017 [hep-ph/0408002].
- [34] O. Buchmuller and H. Flacher, heavy quark expansions in the kinetic scheme,” Phys. Rev. D **73** (2006) 073008 [hep-ph/0507253].
- [35] P. Gambino and C. Schwanda, Phys. Rev. D **89** (2014) 1, 014022 [arXiv:1307.4551 [hep-ph]].
- [36] P. Gambino and S. Turczyk, in Preparation
- [37] J. Heinonen and T. Mannel, Nucl. Phys. B **889** (2014) 46 [arXiv:1407.4384 [hep-ph]].
- [38] T. Aushev *et al.*, arXiv:1002.5012 [hep-ex].
- [39] F. U. Bernlochner, Z. Ligeti and S. Turczyk, Phys. Rev. D **85** (2012) 094033 [arXiv:1202.1834 [hep-ph]].
- [40] A. J. Buras, K. Gemmler and G. Isidori, Nucl. Phys. B **843** (2011) 107 [arXiv:1007.1993 [hep-ph]].
- [41] A. Crivellin, Phys. Rev. D **81** (2010) 031301 [arXiv:0907.2461 [hep-ph]].
- [42] B. M. Dassinger, R. Feger and T. Mannel, Phys. Rev. D **75** (2007) 095007 [hep-ph/0701054].
- [43] B. Dassinger, R. Feger and T. Mannel, Phys. Rev. D **79** (2009) 075015 [arXiv:0803.3561 [hep-ph]].
- [44] R. Feger, T. Mannel, V. Klose, H. Lacker and T. Luck, Phys. Rev. D **82** (2010) 073002 [arXiv:1003.4022 [hep-ph]].
- [45] S. Faller, T. Mannel and S. Turczyk, Phys. Rev. D **84** (2011) 014022 [arXiv:1105.3679 [hep-ph]].
- [46] R. Aaij *et al.* [LHCb Collaboration], Nature Phys. **11** (2015) 743 [arXiv:1504.01568 [hep-ex]].
- [47] F. U. Bernlochner, Z. Ligeti and S. Turczyk, Phys. Rev. D **90** (2014) 9, 094003 [arXiv:1408.2516 [hep-ph]].
- [48] A. Crivellin and S. Pokorski, Phys. Rev. Lett. **114** (2015) 1, 011802 [arXiv:1407.1320 [hep-ph]].
- [49] S. Faller, T. Feldmann, A. Khodjamirian, T. Mannel and D. van Dyk, Phys. Rev. D **89** (2014) 1, 014015 [arXiv:1310.6660 [hep-ph]].
- [50] X. W. Kang, B. Kubis, C. Hanhart and U. G. Meiner, Phys. Rev. D **89** (2014) 053015 [arXiv:1312.1193 [hep-ph]].
- [51] A. Ali, T. Mannel and T. Morozumi, Phys. Lett. B **273** (1991) 505.